Heliyon 11 (2025) e40590

Contents lists available at ScienceDirect

Heliyon

journal homepage: www.cell.com/heliyon

Research article

High glucose induces podocyte ferroptosis through BAP1/SLC7A11 pathway

Ren Peiyao [a,b], Man Xueli [a], Sun Wenbo [a], Zheng Danna [c], Gong Jianguang [c], Jin Juan [a,**], He Qiang [a,*]

[a] Department of Nephrology, The First Affiliated Hospital of Zhejiang Chinese Medical University (Zhejiang Provincial Hospital of Traditional Chinese Medicine), Hangzhou, Zhejiang, 310000, PR China
[b] School of Chinese Medicine, Faculty of Medicine, The Chinese University of Hong Kong, Shatin, N.T., Hong Kong SAR, PR China
[c] Urology & Nephrology Center, Department of Nephrology, Zhejiang Provincial People's Hospital (Affiliated People's Hospital, Hangzhou Medical College), Hangzhou, Zhejiang, 310014, PR China

ARTICLE INFO

Keywords:
Diabetic nephropathy
Ferroptosis
SLC7A11
Ubiquitination

ABSTRACT

Background: Ferroptosis plays an important role in the development of diabetic nephropathy (DN). However, its specific regulatory mechanisms remain unclear.
Methods: MPC5 cells were cultured in high glucose (HG) medium to stimulate the HG environment in vitro. Ferroptosis and oxidative stress were assessed by measuring malondialdehyde (MDA) levels, cystine uptake capacity, and reactive oxygen species (ROS). C91A and wild type (WT) MPC5 cells were constructed to further explore the specific regulatory mechanism of BAP1 on SLC7A11.
Results: Erastin-induced ferroptosis was sensitized by HG, leading to a significant reduction in glutathione (GSH) levels, increased oxidative stress, and inhibited cystine uptake in podocytes. HG suppressed the expression of SLC7A11. Overexpression of SLC7A11 improved cystine uptake and reduced oxidative stress. Furthermore, HG increased BAP1 levels. Silencing BAP1 upregulated SLC7A11 and mitigated ferroptosis. Cell proliferation was reduced after SLC7A11 knockdown. In BAP1 WT cells, but not in its C91A mutant cells, the transcription of SLC7A11 was downregulated and the level of ferroptosis was increased.
Conclusion: HG inhibits cystine uptake in podocytes by promoting the expression of BAP1 and inhibiting H2Aub deubiquitination on SLC7A11, leading to lipid peroxide accumulation and ferroptosis in podocytes.

1. Introduction

Diabetic nephropathy (DN) is a significant complication of diabetes mellitus (DM), accounting for approximately 30%–40 % of diabetic patients [1,2]. Since 2011, DN has gradually surpassed glomerulonephritis as one of the leading causes of end-stage renal failure (ESRD), placing a heavy burden on society [3].

* Corresponding author.
** Corresponding author.
E-mail addresses: renpeiyao1997@163.com (R. Peiyao), Sherry_mang@163.com (M. Xueli), sunwenbo0921@163.com (S. Wenbo), donna_zdn@163.com (Z. Danna), gojigu311@163.com (G. Jianguang), lang_018@163.com (J. Juan), qianghe1973@126.com (H. Qiang).

https://doi.org/10.1016/j.heliyon.2024.e40590
Received 4 June 2024; Received in revised form 15 September 2024; Accepted 19 November 2024
Available online 3 December 2024

Chronic hyperglycaemia can cause both microangiopathy and macroangiopathy, leading to renal damage through oxidative stress [4,5]. The accumulation of reactive oxygen species (ROS) and iron overload have also been implicated in the onset and progression of chronic kidney disease (CKD) [6]. Oxidative stress in podocytes can hinder nephrin expression and decrease adhesion force between podocytes and the glomerular basement membrane, resulting in podocyte shedding, glomerular basement membrane damage, and proteinuria [7]. However, the underlying mechanism has not been fully elucidated.

Iron is essential for DNA synthesis, oxygen transport and redox reactions, as well as maintaining normal cell function, including kidney function [8,9]. Excess iron can generate ROS through the Fenton reaction, contributing to the onset and progression of DN [10]. Studies have shown that streptozotocin-induced diabetic mice and human renal tubular epithelial cells (HK-2) cultured in high glucose (HG) conditions exhibit iron overload, reduced antioxidant capacity, high levels of ROS, and lipid peroxidation in their kidneys. However, diabetic rats fed a low-iron diet or treated with an iron chelator showed delayed progression of DN [11].

Ferroptosis is an iron-dependent form of cell death characterized by excessive iron deposition, ROS production, and lipid peroxidation. GPX4, a key regulator of ferroptosis, can reduce lipid peroxides to lipid alcohols with the help of reduced glutathione, protecting cells from oxidative stress and inhibiting ferroptosis [12,13]. Brca1-associated protein 1 (BAP1) is a deubiquitinating enzyme involved in DNA damage repair, chromatin modification, programmed cell death, and immune response, and plays a role in the epigenetic regulation of gene transcription [14,15]. As a tumor suppressor, BAP1 can target SLC7A11, reduce the H2Aub occupancy on the SLC7A11 promoter, inhibit the function of the amino acid transport complex system Xc-, and induce cancer cell death by promoting lipid peroxidation in cancer cells [16].

Herein, we elucidated the role of ferroptosis in the DN progression at the cellular level, and further clarified the specific molecular mechanism of BAP1 in the DN development.

2. Materials and methods

2.1. Cell culture and treatment

Mouse podocyte cells (MPC5) were purchased from iCell Bioscience (iCell-m081, Shanghai, China). The MPC5 cells were amplified in low-glucose Dulbecco's Modified Eagle's Medium (DMEM, Gibco, San Diego, CA, USA) containing with 10 % FBS and 1 % Penicillin-Streptomycin Liquid (Gibco, San Diego, CA, USA) at 37 °C in a humidified incubator with 5 % CO_2. To mimic the HG condition in vitro, MPC5 cells were treated with 25 mM D-glucose for 48 h after serum-free starvation culture for 8 h. A normal glucose (NG) environment was simulated using 5 mM D-glucose. To investigate the role of ferroptosis, cells were treated with 10 μM erastin, a ferroptosis inducer, for 24 h.

2.2. Lentivirus transduction

The lentiviral vectors (sgBAP1, WT, C91A) were obtained from Professor Zhang Yilei of Xi'an Jiaotong University. After infecting the cells with filtered lentivirus particles for 24 h, selection antibiotic was added to obtain the stably-expressed cells. The oligonucleotides information was listed in Supplementary Table 1.

shRNA targeting SLC7A11 were designed and synthesized by Beijing Tsingke Biotech Co., Ltd. After successful extraction and validation of the plasmid, Lipofectamine Transfection Reagent (Thermo Fisher scientific,18324012) was applied to promote the transfection. The fluorescence intensity was observed with microscope to determine the transfection efficiency, and the expression level of target gene was determined by Western blotting with corresponding antibody.

2.3. Cell viability assay

Cell viability was assessed using the Cell Counting Kit-8 (CCK-8, GLPBIO, GK10001, USA) according to the manufacturer's instructions. Cells were seeded at 5×10^3 cells per well in a 96-well plate. After 8 h of serum-free starvation, cells were treated accordingly for 48 h, and then 10 μL of CCK8 reagent was added to the wells and incubated at 37 °C for 2 h. Absorbance was read at 450 nm using a microplate reader (Bio-Rad Laboratories, Inc.).

2.4. Measurement of malondialdehyde (MDA) levels

Lipid peroxidation was determined by measuring MDA levels using the Lipid Peroxidation MDA Assay Kit (Beyotime). Briefly, cells were lysed, and the supernatant was collected. The MDA concentration was determined by mixing the supernatant with thiobarbituric acid (TBA) and measuring the absorbance at 532 nm.

2.5. Lipid peroxidation detection

Intracellular reactive oxygen species (ROS) levels were measured using the BODIPY 581/591C11(Invitrogen). Briefly, cells in six-well plates were incubated with 1 mL of fresh medium containing 5 μM of BODIPY 581/591C11 for 20 min. Cells were then trypsinized, washed with PBS for three times, and resuspended in 0.5 mL of PBS for flow cytometry analysis.

2.6. Determination of reduced glutathione (GSH) levels

According to the instructions for the GSH and GSSG Assay Kit (S0053, Beyotime,
Shanghai, China), the cells were rinsed with phosphate-buffered saline (PBS, Biosharp, Beijing, China) and then centrifuged for collection. After the mixture of protein removal reagent and the cells were fully Vortex, the cells were frozen and thawed twice in liquid nitrogen and a 37 °C water bath. The supernatant was collected for the determination of total glutathione after centrifugation at 10,000 g for 10 min at 4 °C. The samples and total glutathione test solution were added to the 96-well plate according to the instructions. After thorough mixing, the samples were incubated at room temperature for 5 min. NADPH solution was then added. The absorbance at 412 nm was measured with an enzyme reader after incubation at room temperature for 25 min.

2.7. Cystine uptake assay

Cystine Uptake Assay Kit (DOJINDO, Japan, UP05) was used to detected the activity of xCT by measuring the fluorescence intensity generated by the cystine analogs that had entered the cells. Briefly, cells were seeded into 96-well plates and cultured overnight at 37 °C. After cultured with warmed serum-free and cystine-free medium (Gibco, 21013024) for 5min, warmed CA uptake solution was added to each well, and then cells were cultured in a 5 % CO_2 incubator at 37 °C for 30 min. Then 50 μL methanol and 200 μL working solution was added to each well. The mixture was blown and mixed before standing in the incubator for 30 min. The fluorescence intensity was measured at an excitation wavelength of 490 nm and an emission wavelength of 535 nm using a fluorescence microplate reader.

2.8. Western blotting

Cells were lysed with RIPA buffer, and protein concentrations were determined using the BCA Protein Assay Kit (Beyotime). Equal amounts of protein (30 μg) were separated by SDS-PAGE and transferred onto PVDF membranes. After blocking with 5 % milk, the membrane was incubated with primary antibodies at 4 °C. Secondary antibodies were incubated with the membranes for 1 h at room temperature. An electrochemiluminescence kit was used to visualize the chemiluminescence. The antibody used including Ubiquityl-Histone H2A antibody (CST, #8240, 1:2000), xCT/SLC7A11 antibody (CST#98051, 1:1000), BAP1 antibody (Santa Cruz, sc-28383, 1:1000), β-actin (Proteintech, 81115-1-RR, 1:1000).

2.9. RNA extraction and RT-qPCR

TRIzol reagent (Invitrogen) was used to extract RNAfrom cells. cDNA Synthesis kit (Thermo Fisher Scientific, Inc.) was used to synthesized cDNA. RT-qPCR was performed with SYBR® Green Premix PCR Master Mix (Roche Diagnostics, Indianapolis, IN, USA). The sequences of the primers used are showed in Supplementary Table 2.

2.10. Statistical analysis

Data was statistically analyzed with Prism 9.0. Quantitative data were presented as means ± standard deviation (SD). One-way analysis of variance and *t*-test was used for statistical analysis between groups. Differences were considered significant at $P < 0.05$.

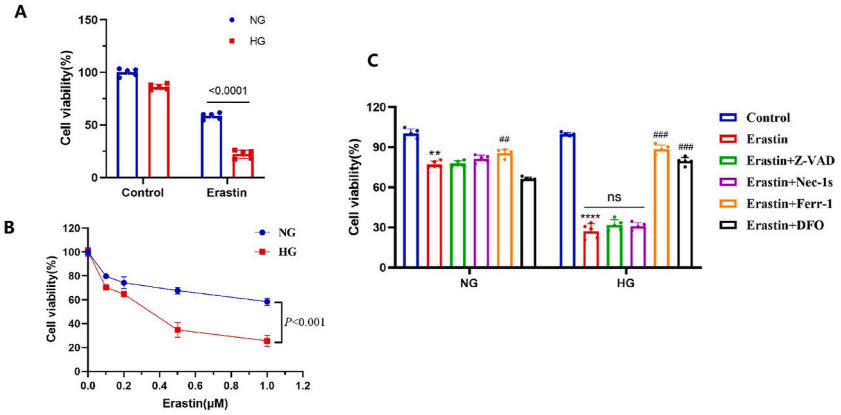

Fig. 1. The impact of HG on the Erastin-induced feroptosis in MPC5.
A. CCK8 was used to detect the cell viability of MPC5 cells in each group. **B.** CCK8 was used to detect the effect of different Erastin concentrations on the viability of MPC5 cells under NG and HG culture conditions. **C.** CCK8 was used to detect the cell viability of MPC5 cells in each group. (The data were presented by Mean ± SD, and one-way ANOVA was used to detect statistical differences between groups, **p < 0.01 VS. Control, ****p < 0.0001 VS. Control, ##p < 0.01 VS. Erastin, ###p < 0.001 VS. Erastin).

3. Results

3.1. HG sensitizes erastin induced ferroptosis in MPC5 cells

Fig. 1A shows that HG (25 mM D-glucose) slightly inhibited the growth of MPC5 cells compared to the effect of low glucose (5 mM D-glucose), but this effect was not significant. However, after erastin treatment, the cell viability of MPC5 cells cultured in HG was significantly lower than that in the NG concentration group. To further explore the effect of concentration of erastin, we pretreated podocytes with different concentrations of erastin and found that the sensitization effect of erastin-induced podocyte death under HG condition was more significant with the increase of erastin concentration (Fig. 1B). To further explore the specific death program of erasin-induced cell death, we applied apoptosis inhibitor (Z-VAD), necrosis inhibitor (Nec-1s) and ferroptosis inhibitors Ferr-1 and DFO on the basis of erastin intervention. Both ferroptosis inhibitors were able to significantly ameliorate erastin-induced cell death (Fig. 1C), demonstrating that ferroptosis was enhanced in HG-sensitized erastin-induced podocytes.

3.2. HG promotes ferroptosis by inhibiting cystine uptake in MPC5 cells

Typical ferroptosis is closely related to cystine transporter function on the cell membrane. GSH level and cystine uptake capacity are important indicators for the occurrence and development of ferroptosis. GSH levels and cystine uptake capacity of MPC5 cells were examined to determine the specific mechanism by which HG regulates podocyte ferroptosis. The results showed that HG intervention significantly reduced the intracellular GSH level and inhibited the cystine uptake capacity of MPC5 cells compared with NG group (Fig. 2A–B). The decrease of GSH level caused by the imbalance of cystine transport capacity will further lead to the imbalance of redox homeostasis, which is also an important regulatory pathway in ferroptosis metabolic disorders. Therefore, MDA level and ROS level of podocytes were detected, and the results showed that compared with the NG group, HG culture could significantly increase the MDA level of podocytes, and enhance the increasing effect of erastin on MDA (Fig. 2C). BODIPY C11 results also showed that HG could promote ferroptosis-specific ROS generation (Fig. 2D). These results indicate that HG can induce oxidative stress and lead to ferroptosis by inhibiting cystine uptake in podocytes.

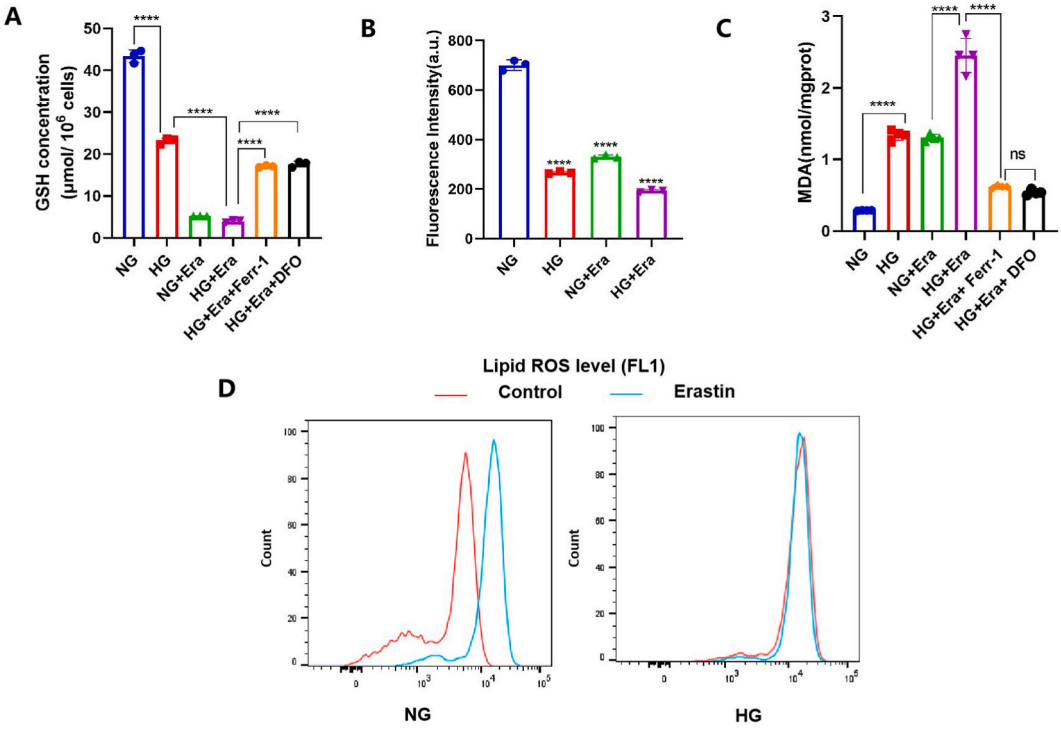

Fig. 2. Effect of HG on cystine uptake capacity and oxidative stress levels in MPC5 cells.
A. GSH assay to detect the GSH level of MPC5 cells in each group. **B.** Cystine uptake capacity assay kit to detect the cystine uptake level of MPC5 cells in different groups. **C.** MDA assay kit to detect the MDA content of MPC5 cells in each group. **D.** Flow cytometry to detect intracellular BODIPY C11 level. (Data were presented in Mean ± SD and statistical differences between groups were detected using one-way ANOVA, ****$p < 0.0001$ VS. Control).

3.3. HG inhibited SLC7A11-mediated cystine uptake and promoted ferroptosis in MPC5 cells

SLC7A11, a key protein of the cystine transporter system Xc-, serves as a key upstream regulators of the ferroptosis regulatory network. To investigate the regulatory effect of HG on SLC7A11 expression, we conducted Western Blotting and RT-qPCR analyses, revealing that HG significantly attenuated SLC7A11 expression at both the protein and mRNA levels, (Fig. 3A–B). This suggests that HG likely regulates cystine uptake in podocyte by regulating SLC7A11 expression. Furthermore, SLC7A11-overexpressing podocytes were constructed and the overexpression efficiency was verified at the protein and mRNA levels (Fig. 3C–D). Measurements of cystine uptake capacity and intracellular GSH levels revealed that podocytes overexpressing SLC7A11 exhibited significantly increased cystine uptake capacity, increased intracellular GSH levels and decreased MDA levels compared to the control group under both NG and HG conditions (Fig. 3E–G). These findings suggest that HG inhibits cystine uptake by inhibiting SLC7A11 expression on the cell membrane, thereby influencing the regulation of ferroptosis.

3.4. HG reduced SLC7A11 function by up-regulating BAP1 expression

Through a literature survey, we identified BAP1, a deubiquitinating enzyme, as a crucial regulator of SLC7A11. which can modulate SLC7A11 function by regulating H2Aub levels on its promoter [12]. Based on this, we hypothesized that BAP1 could be an upstream target of SLC7A11 regulated by HG. Western blotting and RT-qPCR analyses revealed that both the protein and mRNA levels of BAP1 were significantly higher in podocytes cultured with HG compared to the NG group. Interestingly, the expression of BAP1did not change notably compared to the Erastin intervention group, while intracellular H2Aub protein expression levels were lower than those in the NG group (Fig. 4A–B). Subsequently, CRSPER-Cas9 technology was used to generate an sgBAP1 MPC5 cell line, and the knockout of BAP1 was verified successful in Fig. 4C. After BAP1 knockdown, both the protein expression and mRNA levels of SLC7A11 increased (Fig. 4D). Further assessments showed that BAP1 deletion suppressed erastin-induced ferroptosis compared to the control group (Fig. 4E–F). The cystine uptake assay showed that the cystine uptake ability was significantly increased after BAP1 knockdown (Fig. 4G), accompanied by increased intracellular GSH levels (Fig. 4H) and reduced intracellular MDA levels (Fig. 4I). These findings collectively indicate that HG regulates podocyte ferroptosis through BAP1. To ascertain that SLC7A11 acts downstream regulator of BAP1, we constructed an shSLC7A11 cell line based on BAP1 knockdown (Fig. 4J–K), and found that knockdown SLC7A11 on the basis of sgBAP1 significantly inhabited cell viability compared to sgBAP1 MPC5 cells (Fig. 4L). These results suggest that HG inhibits SLC7A11 function by promoting BAP1 expression, thereby inducing ferroptosis in podocytes.

3.5. HG promotes ferroptosis by promoting BAP1 deubiquitination of H2Aub on SLC7A11

BAP1 and its related proteins form the polycomb inhibitory deubiquitinase (PR-DUB) complex, whose main role is to remove mono-ubiquitin from ubiquitinated histone 2A at lysine 119 (H2Aub). To investigate how BAP1 regulates SLC7A11 through deubiquitination of H2Aub at the SLC7A11 promoter, we engineered a C91A mutant of BAP1 using sgBAP1 as a base and generated corresponding wild-type (WT) and empty vector (EV) control cell lines. BAP1 was successfully re-expressed in both the C91A mutant and WT cell lines.

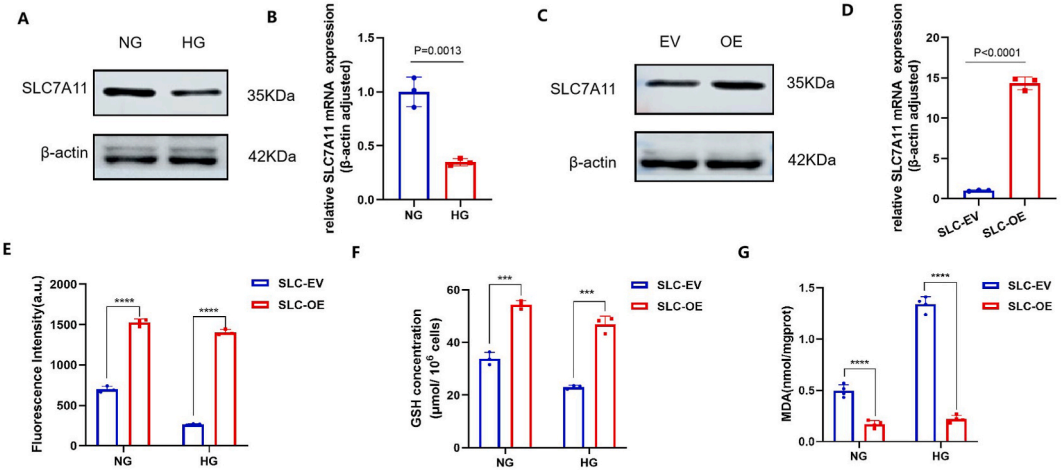

Fig. 3. Effect of HG on SLC7A11 in MPC5 cells and effect of overexpression of SLC7A11 on ferroptosis level in MPC5 cells.
A. WB to detect the SLC7A11 protein expression in MPC5 cells of each group. **B.** RT-qPCR to detect the effect of mRNA level of SLC7A11 in MPC5 cells of each group. **C.** WB to verify the effect of overexpression of SLC7A11 on SLC7A11 protein expression. **D.** RT-qPCR to detect the effect of overexpression of SLC7A11 on the mRNA level of SLC7A11 in MPC5 cells. **E.** Cystine uptake capacity assay kit to detect the level of cystine uptake in MPC5 cells of different groups. **F.** GSH assay to detect the level of GSH in MPC5 cells of different groups. **G.** MDA kit to detect the MDA level of MPC5 cells in each group. (Data were presented as Mean ± SD, and one-way ANOVA was used to detect statistical differences between groups, ***$p < 0.001$,****$p < 0.0001$).

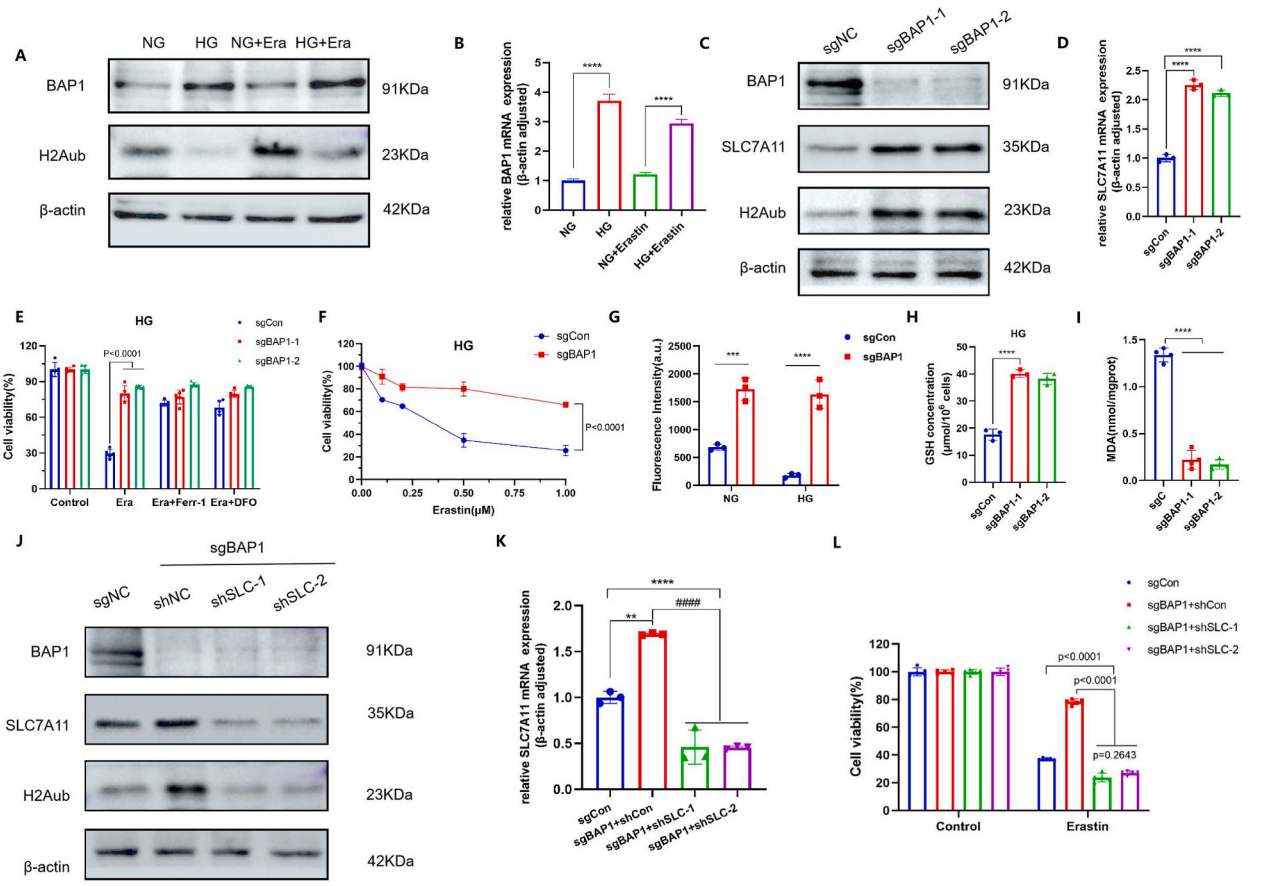

Fig. 4. Effect of BAP1 on SLC7A11 expression and feroptosis in MPC5 cells.
A. WB to detect BAP1 protein expression in each group of MPC5 cells. **B.** RT-qPCR to detect mRNA level of BAP1 in each group of MPC5 cells. **C.** WB tp verify the effect of sgBAP1 on BAP1, SLC7A11 and H2Aub expression **D.** RT-qPCR to detect the effect of sgBAP1 on the mRNA level of SLC7A11 in MPC5 cell. **E.** CCK8 kit to detect the effect of sgBAP1 on the viability of cells in each group. **F.** Cell viability was detected at different erastin concentrations under the HG condition. **G.** Cystine uptake capacity assay kit to detect the cystine uptake level of MPC5 cells in different groups. **H.** GSH assay to detect the GSH level of MPC5 cells in different groups. **I.** MDA assay kit to detect the MDA content of MPC5 cells in different groups. **J.** WB assay to detect the effect of shSLC7A11 on the expression of BAP1, SLC7A11 and H2Aub. **K.** RT-qPCR assay to detect the effect of sgBAP1 on the expression of BAP1, SLC7A11 and H2Aub in different groups. Effect of shSLC7A11 on the mRNA level of SLC7A11 in MPC5 cells. **L.** CCK8 kit to detect the proliferative capacity of cells in each group. (Data were presented as Mean ± SD, and one-way ANOVA was used to detect statistical differences between groups, ***$p < 0.001$,****$p < 0.0001$).

Interestingly, the protein expression level of SLC7A11 in the C91A mutant cell line was significantly higher than in the WT cell line, although there was no notable difference compared to the EV group. This observation suggests that loss of ubiquitinase activity impairs BAP1's ability to regulate SLC7A11 effectively (Fig. 5A–B). Further analysis through cell proliferation assay revealed that the promotive effect of HG on erastin-induced ferroptosis was attenuated in C91A mutant cell lines compared to the WT group (Fig. 5C–D). Additionally, the cystine uptake assay demonstrated that the cystine uptake ability of C91A mutant was significantly higher than that of WT group. Consistently, measurement of GSH levels indicated that the C91A mutant cells had higher GSH levels than the WT cells, while MDA levels were lower in the C91A mutant cell lines compared to the WT group (Fig. 5E–G). These findings collectively indicate that BAP1 regulates SLC7A11 expression through its deubiquitination activity, thereby influencing the level of ferroptosis. The C91A mutation, which abolishes BAP1's ubiquitinase function, leads to enhanced SLC7A11 expression and altered cellular responses to HG and erastin-induced stress, highlighting the intricate regulatory role of BAP1 in cellular ferroptosis pathways (see Fig. 6).

4. Discussion

DN is characterized by multifaceted pathogenic mechanisms including inflammation, autophagy, apoptosis, oxidative stress, and ferroptosis, all of which contribute to podocyte dysfunction and subsequent renal impairment [17]. In recent years, accumulating studies have indicated that oxidative stress and ferroptosis are also important factors in DN [18,19]. In this study, we revealed that HG inhibited the deubiquitination of H2Aub by promoting the expression of BAP1 in podocytes in vitro, resulting in decreased transcription of SLC7A11, a key component of System Xc-, thereby impeding the transport of extracellular cystine into cells and resulting in

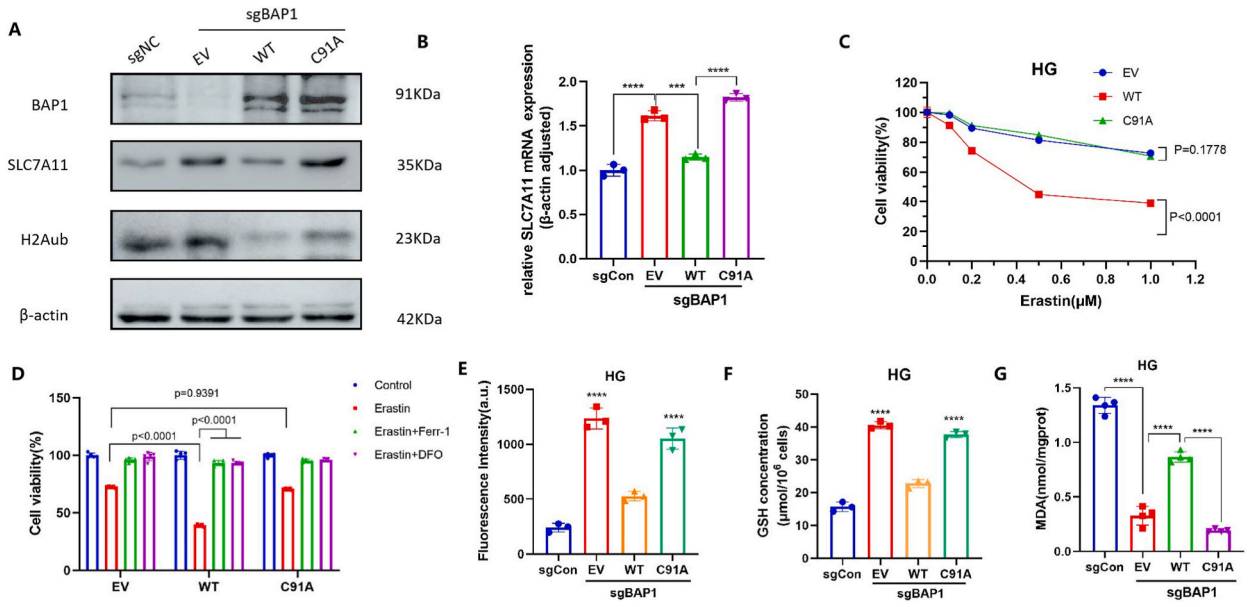

Fig. 5. Effect of deubiquitinating enzyme activity of BAP1 on HG-regulated feroptosis in MPC5 cells.
A. WB to detect BAP1, SLC7A11 and H2Aub protein expression in MPC5 cells of each group. **B.** RT-qPCR assay to detect the effect of mRNA level of SLC7A11 in MPC5 cells of each group. **C.** CCK8 kit assay to detect the effect of increasing erastin concentration on the viability of C91A, WT and EV cells. **D.** CCK8 kit to detect the effect of cell viability in each group. **E.** Cystine uptake capacity assay kit to detect the level of cystine uptake in MPC5 cells of different groups. **F.** GSH to detect the level of GSH in MPC5 cells of each group. **G.** MDA kit to detect the MDA the MDA level of MPC5 cells in each group. (The data were presented in Mean ± SD, and one-way ANOVA was used to detect statistical differences between groups, ***$p < 0.001$VS. sgControl,****$p < 0.0001$VS. sgControl).

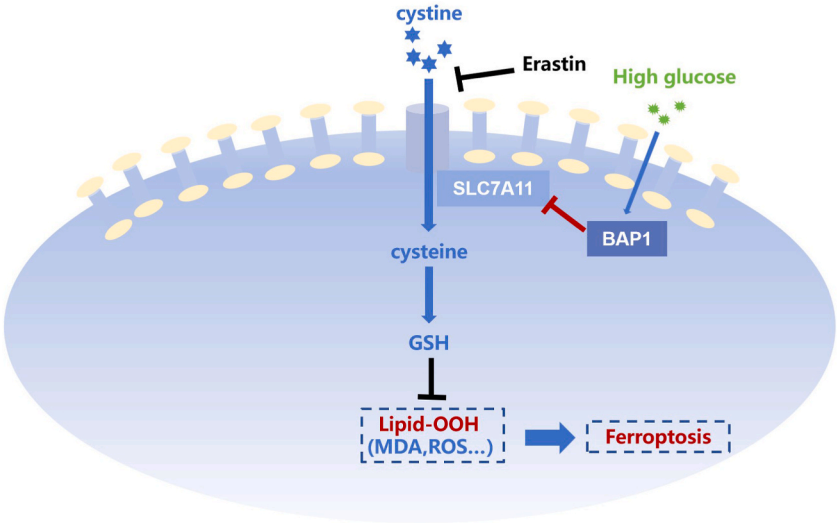

Fig. 6. Model for HG regulated BAP1-SLC7A11 pathway in MPC5.
HG inhibits cystine uptake in podocytes by promoting the expression of BAP1 and inhibiting H2Aub deubiquitination on SLC7A11, leading to the deposition of lipid peroxides and the occurrence of ferroptosis in podocytes.

intracellular lipid peroxide accumulation, which further exacerbates podocyte injury.

Ferroptosis, an iron-dependant form of cell death, is intricately linked to cellular metabolism and levels of ROS, which are influenced by intracellular and intercellular signaling events as well as environmental stresses [20–22]. Oxidative stress arises from an imbalance between ROS production and antioxidant defense mechanisms [23]. Iron, especially in its free form, catalyzes ROS production, leading to oxidative damage in various cell types including hepatocytes, cardiomyocytes, neurons, and kidney cells. Previous studies have found that inhibiting ferroptosis can effectively attenuate the progression from acute kidney injury (AKI) to CKD [24].

Furthermore, ferroptosis inhibitors such as Quercetin have been shown to mitigate AKI by preventing typical morphological changes in ferroptotic cells [25].

The involvement of ferroptosis in DN pathogenesis is increasingly recognized. Dysregulated iron metabolism exacerbates inflammatory responses, thereby promoting the occurrence and development of DN. It has been reported that ferroptosis inhibitors can upregulate nuclear factor-E2-related factor 2 (Nrf2), which plays a crucial role in inhibiting diabetes-related ferroptosis and potentially delaying DN progression [26]. Endoplasmic reticulum stress (ERS), triggers ferroptosis-related EMT progression through the XBP1-Hrd1-Nrf2 pathway in DN progression [27]. However, the underlying molecular biological mechanism by which ferroptosis regulates DN is complex and still remains unclear.

SLC7A11, serves as the principal functional protein of the amino acid transport complex system Xc-, can promote the synthesis of glutathione by mediating cystine uptake and glutamate release. This process protects cells against oxidative stress, maintains cellular redox balance, and prevents cell death triggered by lipid peroxidation, playing a pivotal role in regulating ferroptosis. The transcription of SLC7A11 gene can be regulated by multiple transcription factors [28,29]. Notably, the transcription factor Nrf2 can bind to the promoter region of the SLC7A11 gene and promote its transcription [30]. Additionally, BAP1 has emerged as an important regulator of SLC7A11, which can directly bind to the promoter region of SLC7A11 gene and affect its transcriptional activity [31]. This mechanism has been validated in renal cancer cells, but there is currently no evidence to elucidate the specific regulatory role of BAP1 in DN ferroptosis [32]. This study fills this gap by demonstrating that high glucose regulates podocyte ferroptosis by promoting BAP1 expression and represses SLC7A11 transcription.

In the future, we aim to verify our findings in vivo and explore how HG impacts mitochondrial morphology and function. Additionally, we will delve deeper into the specific mechanisms through which HG regulates BAP1, so as to provide novel insights into the biological pathways involved in targeting ferroptosis as a strategy to inhibit the progression of DN.

5. Conclusion

HG inhibits cystine uptake in podocytes by promoting the expression of BAP1 and inhibiting H2Aub deubiquitination on SLC7A11, a functional protein targeting cystine transporter system Xc-on the cell membrane, leading to the deposition of lipid peroxides and the occurrence of ferroptosis in podocytes.

CRediT authorship contribution statement

Ren Peiyao: Writing – original draft, Formal analysis, Data curation. **Man Xueli:** Writing – review & editing. **Sun Wenbo:** Writing – review & editing. **Zheng Danna:** Writing – review & editing, Funding acquisition, Formal analysis. **Gong Jianguang:** Writing – review & editing, Supervision. **Jin Juan:** Writing – review & editing, Supervision, Project administration, Conceptualization. **He Qiang:** Writing – review & editing, Supervision, Project administration, Data curation.

Data availability

All data supporting the finding are provided in the article and Supplementary materials. More details of this study are available from the corresponding author on reasonable request.

Funding

This research was supported by National Natural Science Foundation of China (82374201); the Huadong Medicine Joint Funds of the Zhejiang Provincial Natural Science Foundation of China (Grant No. LHDMZ22H050001); the Construction of Key Projects by Zhejiang Provincial Ministry (Project No. WKJ-ZJ-2302); The Key Project of Scientific Research Foundation of Chinese Medicine (2022ZZ002); “Pioneer” and “Leading Goose” R&D Program of Zhejiang (2023C03075); Hua tong Guo kang Medical Research Project (2023HT079); Medicine and health science and technology plan projects in Zhejiang province (2023KY533); Project of the State Administration of Traditional Chinese Medicine (2023ZR063).

Declaration of competing interest

The authors declare that they have no relevant financial interests.

Appendix A. Supplementary data

Supplementary data to this article can be found online at https://doi.org/10.1016/j.heliyon.2024.e40590.

References

[1] K. Umanath, J.B. Lewis, Update on diabetic nephropathy: core curriculum 2018, Am. J. Kidney Dis. 71 (6) (2018) 884–895, https://doi.org/10.1053/j.ajkd.2017.10.026.

[2] M. Liu, S.W. Liu, L. Wang, et al., Burden of diabetes, hyperglycaemia in China from to 2016: findings from the 1990 to 2016, global burden of disease study, Diabetes Metabol. 45 (3) (2019) 286–293, https://doi.org/10.1016/j.diabet.2018.08.008.

[3] P. Saeedi, I. Petersohn, P. Salpea, et al., Global and regional diabetes prevalence estimates for 2019 and projections for 2030 and 2045: results from the international diabetes federation diabetes atlas, Diabetes Res. Clin. Pract. 157 (2019) 107843, https://doi.org/10.1016/j.diabres.2019.107843, 9 edition.

[4] Y. An, B.-T. Xu, S.-R. Wan, et al., The role of oxidative stress in diabetes mellitus-induced vascular endothelial dysfunction, Cardiovasc. Diabetol. 22 (1) (2023) 237, https://doi.org/10.1186/s12933-023-01965-7.

[5] M. Darenskaya, S. Kolesnikov, N. Semenova, L. Kolesnikova, Diabetic nephropathy: significance of determining oxidative stress and opportunities for antioxidant therapies, Int. J. Mol. Sci. 24 (15) (2023) 12378, https://doi.org/10.3390/ijms241512378. Published 2023 Aug 3.

[6] J.C. Jha, C. Banal, B.S.M. Chow, et al., Diabetes and kidney disease: role of oxidative stress, Antioxidants Redox Signal. 25 (12) (2016) 657–684, https://doi.org/10.1089/ars.2016.6664.

[7] H. Dai, Q. Liu, B. Liu, Research progress on mechanism of podocyte depletion in diabetic nephropathy, J. Diabetes Res. 2017 (2017) 2615286, https://doi.org/10.1155/2017/2615286.

[8] B. Galy, M. Conrad, M. Muckenthaler, Mechanisms controlling cellular and systemic iron homeostasis, Nat. Rev. Mol. Cell Biol. 25 (2) (2024) 133–155, https://doi.org/10.1038/s41580-023-00648-1.

[9] A.R. Bogdan, M. Miyazawa, K. Hashimoto, Y. Tsuji, Regulators of iron homeostasis: new players in metabolism, cell death, and disease, Trends Biochem. Sci. 41 (3) (2016) 274–286, https://doi.org/10.1016/j.tibs.2015.11.012.

[10] J.M. Fernández-Real, A. López-Bermejo, W. Ricart, Cross-talk between iron metabolism and diabetes, Diabetes 51 (8) (2002) 2348–2354, https://doi.org/10.2337/diabetes.51.8.2348.

[11] S. Li, L. Zheng, J. Zhang, et al., Inhibition of ferroptosis by up-regulating nrf2 delayed the progression of diabetic nephropathy, Free Radic. Biol. Med. 162 (2021) 435–449, https://doi.org/10.1016/j.freeradbiomed.2020.10.323.

[12] W.S. Yang, B.R. Stockwell, Ferroptosis: death by lipid peroxidation, Trends Cell Biol. 26 (3) (2016) 165–176, https://doi.org/10.1016/j.tcb.2015.10.014.

[13] D. Tang, X. Chen, R. Kang, et al., Ferroptosis: molecular mechanisms and health implications, Cell Res. 31 (2) (2021) 107–125, https://doi.org/10.1038/s41422-020-00441-1.

[14] A. Han, T.J. Purwin, A.E. Aplin, Roles of the bap1 tumor suppressor in cell metabolism, Cancer Res. 81 (11) (2021) 2807–2814, https://doi.org/10.1158/0008-5472.CAN-20-3430.

[15] M. Carbone, J.W. Harbour, J. Brugarolas, et al., Biological mechanisms and clinical significance of mutations in human cancer, Cancer Discov. 10 (8) (2020) 1103–1120, https://doi.org/10.1158/2159-8290.CD-19-1220.

[16] Y. Zhang, J. Shi, X. Liu, et al., Bap1 links metabolic regulation of ferroptosis to tumour suppression, Nat. Cell Biol. 20 (10) (2018) 1181–1192, https://doi.org/10.1038/s41556-018-0178-0.

[17] P. Baum, K.V. Toyka, M. Blüher, J. Kosacka, M. Nowicki, Inflammatory mechanisms in the pathophysiology of diabetic peripheral neuropathy (DN)-New aspects, Int. J. Mol. Sci. 22 (19) (2021) 10835, https://doi.org/10.3390/ijms221910835. Published 2021 Oct 7.

[18] J. Li, L. Li, Z. Zhang, et al., Ferroptosis: an important player in the inflammatory response in diabetic nephropathy, Front. Immunol. 14 (2023) 1294317, https://doi.org/10.3389/fimmu.2023.1294317. Published 2023 Dec 4.

[19] Q. Jin, T. Liu, Y. Qiao, et al., Oxidative stress and inflammation in diabetic nephropathy: role of polyphenols, Front. Immunol. 14 (2023) 1185317, https://doi.org/10.3389/fimmu.2023.1185317. Published 2023 Jul 21.

[20] D. Liang, A.M. Minikes, X. Jiang, Ferroptosis at the intersection of lipid metabolism and cellular signaling, Mol. Cell. 82 (12) (2022) 2215–2227, https://doi.org/10.1016/j.molcel.2022.03.022.

[21] S. Sun, J. Shen, J. Jiang, F. Wang, J. Min, Targeting ferroptosis opens new avenues for the development of novel therapeutics, Signal Transduct. Targeted Ther. 8 (1) (2023) 372, https://doi.org/10.1038/s41392-023-01606-1. Published 2023 Sep. 21.

[22] X. Jiang, B.R. Stockwell, M. Conrad, Ferroptosis: mechanisms, biology and role in disease, Nat. Rev. Mol. Cell Biol. 22 (4) (2021) 266–282, https://doi.org/10.1038/s41580-020-00324-8.

[23] Y.A. Hajam, R. Rani, S.Y. Ganie, et al., Oxidative stress in human pathology and aging: molecular mechanisms and perspectives, Cells 11 (3) (2022) 552, https://doi.org/10.3390/cells11030552. Published 2022 Feb 5.

[24] Q. Feng, Y. Yang, K. Ren, et al., Broadening horizons: the multifaceted functions of ferroptosis in kidney diseases, Int. J. Biol. Sci. 19 (12) (2023) 3726–3743, https://doi.org/10.7150/ijbs.85674. Published 2023 Jul 16.

[25] Y. Wang, F. Quan, Q. Cao, et al., Quercetin alleviates acute kidney injury by inhibiting ferroptosis, J. Adv. Res. 28 (2021) 231–243, https://doi.org/10.1016/j.jare.2020.07.007.

[26] S. Li, L. Zheng, J. Zhang, et al., Inhibition of ferroptosis by up-regulating nrf2 delayed the progression of diabetic nephropathy, Free Radic. Biol. Med. 162 (2021) 435–449, https://doi.org/10.1016/j.freeradbiomed.2020.10.323.

[27] Z. Liu, P. Nan, Y. Gong, et al., Endoplasmic reticulum stress-triggered ferroptosis via the xbp1-hrd1-nrf2 pathway induces emt progression in diabetic nephropathy, Biomed. Pharmacother. 164 (2023) 114897, https://doi.org/10.1016/j.biopha.2023.114897.

[28] P. Koppula, L. Zhuang, B. Gan, Cystine transporter SLC7A11/xCT in cancer: ferroptosis, nutrient dependency, and cancer therapy, Protein Cell 12 (8) (2021) 599–620, https://doi.org/10.1007/s13238-020-00789-5.

[29] J. Lee, J.L. Roh, SLC7A11 as a gateway of metabolic perturbation and ferroptosis vulnerability in cancer, Antioxidants 11 (12) (2022) 2444, https://doi.org/10.3390/antiox11122444. Published 2022 Dec 11.

[30] L. Feng, K. Zhao, L. Sun, et al., SLC7A11 regulated by NRF2 modulates esophageal squamous cell carcinoma radiosensitivity by inhibiting ferroptosis, J. Transl. Med. 19 (1) (2021) 367, https://doi.org/10.1186/s12967-021-03042-7. Published 2021 Aug 26.

[31] Y. Zhang, P. Koppula, B. Gan, Regulation of H2A ubiquitination and SLC7A11 expression by BAP1 and PRC1, Cell Cycle 18 (8) (2019) 773–783, https://doi.org/10.1080/15384101.2019.1597506.

[32] L. Masclef, O. Ahmed, B. Estavoyer, et al., Roles and mechanisms of BAP1 deubiquitinase in tumor suppression, Cell Death Differ. 28 (2) (2021) 606–625, https://doi.org/10.1038/s41418-020-00709-4.